Bioresource Technology Reports 23 (2023) 101592

Contents lists available at ScienceDirect

Bioresource Technology Reports

journal homepage: www.sciencedirect.com/journal/bioresource-technology-reports

Ammonium nitrogen (NH_4^+-N) recovery from synthetic wastewater using biosolids-derived biochar

Pobitra Halder [a,b,c,*], Mojtaba Hedayati Marzbali [a,b], Savankumar Patel [a,b], Graeme Short [d], Aravind Surapaneni [b,d], Rajender Gupta [e], Kalpit Shah [a,b]

[a] Chemical and Environmental Engineering, School of Engineering, RMIT University, Melbourne, VIC 3000, Australia
[b] ARC Training Centre for the Transformation of Australia's Biosolids Resources, RMIT University, Bundoora, VIC 3083, Australia
[c] School of Engineering, Deakin University, VIC 3216, Australia
[d] South East Water Corporation, Frankston, VIC 3199, Australia
[e] Department of Chemical and Materials Engineering, University of Alberta, Edmonton T6G 2H5, Canada

ARTICLE INFO

Keywords:
Nutrient recovery
Biosolids biochar
Adsorption
Functional groups
Cation exchange
Circular economy

ABSTRACT

The nutrient removal in the wastewater treatment plant is a critical step before the treated water is either recycled or discharged into natural water bodies. The current work provides a low-cost and environmentally sustainable nitrogen recovery approach from wastewater using biosolids-derived biochar. The biochar, produced from the pyrolysis of biosolids, was tested for NH_4^+-N adsorption from a synthetic wastewater sample via a batch adsorption experiment and compared with biomass-derived biochar, cation exchange resin, zeolite, and activated carbon. The adsorption capacity of biochar produced at 500 °C was around 1.8 mg g^{-1} for an initial NH_4^+-N concentration of 50 mg L^{-1}, which was half of the cation exchange resin and zeolite given the presence of sulfonate (-SO_3H) and -OH groups on their surface to exchange H^+ ion with NH_4^+-N ion. The external surface layer and intra-particle diffusion were the rate-controlling steps of the adsorption process, as reflected in the kinetic modelling results, where a pseudo first-order model could best describe the evolution of adsorption. The presence of active sites with varied affinities towards NH_4^+-N adsorption on the heterogeneous surface of the adsorbent and the occurrence of multilayer adsorption were implied by the acceptable fitting of isotherm experimental data to Freundlich and Temkin models, respectively. Biosolids-derived biochar may be an attractive adsorbent for ammonium recovery from wastewater in a circular economy concept.

1. Introduction

The wastewater that enters the wastewater treatment plant (WWTP) mainly consists of domestic and industrial wastewater. Domestic wastewater includes urine stream, faeces, grey water, and toilet flushing water (van der Hoek et al., 2018). Human urine contains approximately 85–90 % of nitrogen, 80–90 % of potassium, and 50–80 % of phosphorus present in domestic wastewater (Xu et al., 2018). Nitrogen in human fresh urine typically presents in the form of urea, which gets converted to ammonium nitrogen (NH_4^+-N) due to the bacteria present in urine and ammonia (NH_3) gas through enzymatic hydrolysis. The influent (urine and other wastewater streams) in the WWTP contains nitrogen dominantly in the form of NH_4^+-N (Kundu et al., 2022). In the WWTP, NH_4^+-N in wastewater is converted to nitrate nitrogen (NO_3^--N) and nitrite nitrogen (NO_2^--N) which is further converted to N_2 gas through nitrification-denitrification processes and released N_2 back to the atmosphere (Beckinghausen et al., 2020; Rahimi et al., 2020).

The nutrient removal in WWTP is a critical step before the treated water is either recycled or discharged into natural water bodies (Pronk and Koné, 2009). The regulations are becoming more stringent recently and limits to nutrient discharge have been reduced significantly in the last three decades (Pronk and Koné, 2009). For instance, the regulatory limits for discharging nitrogen in rivers in Australia are ≤1 mg L^{-1} ammonia and ≤50–100 mg L^{-1} total nitrogen, depending on the site and those in China are ≤5 mg L^{-1} ammonium and ≤15 mg L^{-1} total nitrogen (AMPC, 2022; Du et al., 2015). The US EPA has imposed a nitrogen discharge limit of 1–3 mg L^{-1} (Nayak et al., 2021). For WWTP, it is becoming extremely hard to keep the wastewater treatment at low costs with changing regulations and increased nutrient loading and contaminants in the wastewater (Preisner et al., 2021). More importantly, the

* Corresponding author at: Chemical and Environmental Engineering, School of Engineering, RMIT University, Melbourne, VIC 3000, Australia.
E-mail address: pobitra.halder@rmit.edu.au (P. Halder).

https://doi.org/10.1016/j.biteb.2023.101592
Received 18 May 2023; Received in revised form 11 August 2023; Accepted 13 August 2023
Available online 15 August 2023

current focus of most of the water utilities is on nutrient removal and not nutrient recovery in their existing treatment process. Therefore, considering the stringent discharge regulations, rapid increase in nitrogen-based fertiliser demand, and associated environmental emissions (~935 million tons CO_2 annually (Safie and Zahrim, 2021)), the focus has been shifted to nitrogen recovery.

The existing nutrient recovery methods available or currently under development for recovering nitrogen from wastewater such as ammonia stripping, electrochemical methods, and membrane-based technologies are either expensive or require significant infrastructure upgradation in the existing WWTP (Kundu et al., 2022). Therefore, water industries are looking for an alternative low-cost technology, which can be installed without any significant changes in the existing process and infrastructure and support the circular economy.

The sorption-based techniques using cation exchange resin, zeolite, and activated carbon adsorbent are considered promising wastewater treatment options due to their several advantages, such as accessibility, simplicity in operation, feasible reactor designs and economics over other technologies, and have proven suitability for nitrogen recovery from wastewater (Bhatnagar and Sillanpää, 2011). Cation exchange resin and zeolite are the most common commercial adsorbents, which have been investigated widely for nitrogen recovery from wastewater (Chen et al., 2019; Han et al., 2021; Safie and Zahrim, 2021; Sánchez and Martins, 2021; Tarpeh et al., 2018) and exhibited 0.7–85 mg g^{-1} and 0.24–23.7 mg g^{-1} nitrogen adsorption, respectively, depending on the type of adsorbent, initial nitrogen concentration and adsorption process conditions.

Recently, biochar-based sorption techniques have received immense research interest to the scientific community and water industries for nutrient recovery from wastewater due to several advantages (Chang et al., 2023; Li et al., 2021; Zhao et al., 2022): (i) it is produced from widely available feedstocks through a simple process, (ii) its low production cost lowers the overall biochar cost, (iii) it has excellent physico-chemical properties, including high functional groups, cation exchange capacity, carbon content and porosity and (iv) it can fix up to ~2.57 tons of CO_2 per ton of biochar. Apart from these, nitrogen-loaded biochar can be used as a nitrogen-based fertiliser for soil conditioning which can enhance crop growth (Shang et al., 2018) and reduce the dependency on the synthetic nitrogen fertiliser.

So far, biomass-derived biochars have been widely investigated to recover nitrogen in the form of ammonium from synthetic wastewater (mainly representing flushed urine stream) or real urine (Chang et al., 2023; Chen et al., 2021; Dai et al., 2020; Li et al., 2021; Shang et al., 2018; Simha et al., 2018; Wang et al., 2022, 2020; Xu et al., 2018; Xue et al., 2019; Yin et al., 2017). The use of biosolids biochar, produced from biosolids in the WWTP premises, instead of biomass biochar can bring more benefits to the water industries by avoiding the transport cost of biochar from the pyrolysis plant to WWTP site and managing biosolids in a circular way. The physico-chemical properties of biosolids-derived biochar may significantly be different from those of biomass-derived biochar which indicates the need for studying biosolids-derived biochar-based adsorption process.

To this point, only a few studies have focused on using biosolids or sewage sludge or faecal sludge-derived biochar for nitrogen recovery (Bai et al., 2018; Beckinghausen et al., 2020; Carey et al., 2015; Li et al., 2018; Tang et al., 2019). However, these studies exhibited nitrogen recovery from ammonium-only solution, which is not representative of wastewater. A recent study (Yu, 2022) used dewatered municipal sludge-derived biochar for NH_4^+-N recovery from real fresh urine (not representative of wastewater) without any benchmarking of sludge-derived biochar with other adsorbents. Therefore, it would be interesting to investigate how biosolids-derived biochar performs for NH_4^+-N adsorption from real wastewater or synthetic wastewater compared to the well-studied biomass-derived biochar and other commercial adsorbents. The role of other adsorbate molecules in wastewater on NH_4^+-N adsorption using biosolids-derived biochar is still unknown.

Therefore, the present study is looking to recover nitrogen from wastewater at a centralised level using biochar derived from biosolids and biomass. The idea is to then directly use this nitrogen-loaded biochar as a fertiliser for land application. The aims of the current work are to (i) investigate the performance of biosolids-derived biochar for ammonium adsorption from synthetic wastewater, representative to real wastewater at WWTP, (ii) benchmark the biosolids-derived biochar against zeolite, ion exchange resin, biomass biochar and activated carbon for ammonium adsorption, (iii) study the effects of heavy metals and drugs on the ammonium adsorption performance of biosolids-derived biochar and (iv) derive adsorption kinetics and isotherms for biosolids-derived biochar adsorbent. The current work represents a truly circular economy concept and is expected to be an environmentally sustainable and cost-efficient method for nitrogen recovery from wastewater.

2. Materials and methods

2.1. Materials and chemicals

Biosolids were supplied by the Southeast Water Mount Martha WWTP, Victoria, Australia. Oak wood was purchased from a local store in Victoria, Australia. Zeolite, activated carbon, Caffeine, and Zinc precursors were purchased from Sigma Aldrich, Australia. Cation exchange resin (AG® 50 W-X8, 200–400 dry mesh size, 63–150 μm wet bead size, 8 % cross-linkage, hydrogen form) was purchased from Bio-Rad, Australia. Primary effluent at WWTP was synthesised using the composition in Table 1 as reported in the literature. The concentrations of the wastewater compositions were similar to the average concentration in primary effluent from South East Water treatment plant. Ammonium chloride (NH_4Cl) was added to the synthetic wastewater solution to prepare various concentrations of ammonium. All these chemicals as wastewater constituents were purchased from Sigma Aldrich, Australia in analytical grade and used as received.

2.2. Biochar preparation and characterisation of adsorbents

2.2.1. Biochar production

Biochar samples from biosolids and biomass (Oak wood) were produced via slow pyrolysis. Biosolids and biomass were dried in an oven at 105 °C for 24 h, and ground in a mill to the size range of 300 to 500 μm for biochar production. The pyrolysis experiments were conducted in a muffle furnace (Barnstead Thermolyne 30400). The biosolids and biomass samples were then weighed into crucibles with tight lids and placed in the muffle furnace. Biosolids and biomass samples were heated in the furnace at a heating rate of 20 °C min^{-1} to pyrolysis temperature (500 and 700 °C) under a nitrogen environment and the samples were kept at pyrolysis temperature for 3 h. The biochar samples inside the furnace were then cooled down naturally to room temperature avoiding any exposure of air to the hot samples. The cooled biochar samples were collected and weighted for biochar yield estimation and finally stored in

Table 1
Composition of the synthetic wastewater (Pramanik et al., 2020).

Component	Concentration (mg L^{-1})
Glucose	100
Peptone	100
Potassium dihydrogen phosphate	17.5
Magnesium sulphate	17.5
Sodium acetate	225
Ferrous sulphate	10
Sodium chloride	150
Sodium nitrate	10
Calcium carbonate	100
Kaolinite	10
Urea	35

a desiccator for characterisation and adsorption experiments. The biochar yield was estimated as ~40–45 %, depending on the feedstock and temperature.

Biochar characteristics may be significantly affected by any fluctuation in pyrolysis temperature (Širić et al., 2022); therefore, delicate self-control of the whole process conditions is needed. Biosolids pyrolysis at 400 °C exhibited significantly lower carbonisation compared to that of 500 °C, as observed in the Authors' previous study (Patel et al., 2019). The lack of sufficient carbonisation of biosolids during pyrolysis is expected to lower the NH_4^+-N adsorption capacity of biochar produced from the respective pyrolysis temperature (Tang et al., 2019). Therefore, the current study considered biochars produced from the pyrolysis of biosolids at 500 and 700 °C.

2.2.2. Adsorbents characterisation

The surface functional groups of adsorbents were analysed using Fourier-transform infrared spectroscopy (FTIR) spectra of the adsorbents. The FTIR spectroscopic analyses of adsorbents were performed in absorbance mode with a wavenumber range of 4000–600 cm^{-1} using a PerkinElmer FTIR Spectrometer (Spectrum 100, USA).

The Brunauer–Emmett–Teller (BET) surface areas of adsorbents were estimated from the nitrogen gas adsorption–desorption isotherm data of the adsorbents using a Micromeritics ASAP 2400 instrument at 77 K. Before adsorption–desorption isotherm analysis, the adsorbent samples were first degassed at room temperature in slow-mode for 30 min under vacuum and then at 150 °C in fast-mode for 24 h under vacuum.

2.3. Batch adsorption experiments

2.3.1. Benchmarking experiments

NH_4^+-N adsorption experiments from the synthetic wastewater were performed at room temperature using biosolids/biomass-derived biochar. NH_4^+-N adsorption performance of biosolids/biomass-derived biochar adsorbent was compared and benchmarked with other adsorbents (i.e., zeolite, activated carbon, and ion exchange resin) for nitrogen recovery from the synthetic wastewater. The experiments were performed for initial NH_4^+-N concentrations of 5 and 50 mg L^{-1} and contact time of 5 and 24 h with a shaking speed of 180 rpm. All adsorption experiments were conducted by adding 1 g of each adsorbent to 100 ml of the prepared wastewater. After adsorption, the solution was centrifuged, and the supernatant was analysed using HACH Nitrogen-Ammonia Reagent Set, TNT, Am*V*er (Salicylate), High Range kit to determine the concentration of NH_4^+-N. The capacity of adsorbents for ammonium adsorption and ammonium removal efficiency were calculated using the following equations (Al nami and Hossan, 2023):

$$Q_e = \frac{(C_0 - C_{tf})V}{m} \quad (1)$$

$$\text{Removal efficiency } (\%) = \frac{C_0 - C_{t_f}}{C_0} \times 100 \quad (2)$$

where Q_e is the adsorption capacity (mg g^{-1}), C_0 and C_{tf} (mg L^{-1}) are the initial and final ammonium concentration in the aqueous phase respectively, V denotes the batch volume (L^{-1}), and m is the dried weight of adsorbent (g).

2.3.2. Investigating the role of other adsorbate molecules

NH_4^+-N adsorption performance of biosolids-derived biochar from the synthetic wastewater was further investigated in the presence of heavy metal (Zinc) and drug (Caffeine), as only Zinc and Caffeine were in considerable concentration in South East Water primary effluent. The experiments were performed at 50 mg L^{-1} NH_4^+-N concentration for 24 h with shaking at 180 rpm. The concentration of Zinc and Caffeine was maintained at 0.05 mg L^{-1}, considering the concentration in real wastewater.

2.3.3. Adsorption experiments for kinetics study

NH_4^+-N adsorption kinetics data were correlated for biosolids-derived biochar using different models. The experiments were conducted at room temperature using synthetic wastewater of NH_4^+-N concentration of 50 mg L^{-1} for different adsorption times ranging from 0.5 to 24 h with shaking at 180 rpm.

2.3.4. Adsorption experiments for isotherms study

NH_4^+-N adsorption isotherms were derived for biosolids-derived biochar using different isotherm relations such as Langmuir, Temkin, and Freundlich models. The experiments were conducted at room temperature using synthetic wastewater of different initial NH_4^+-N concentrations ranging from 5 to 100 mg L^{-1} for 24 h with shaking at 180 rpm. Adsorption time was selected as 24 h for ensuring the equilibrium.

2.4. Adsorption kinetics and isotherms models

In this study, four kinetic models such as Pseudo first order, Pseudo second order, Elovich, and intra-particle diffusion models and three isotherm modes such as Freundlich, Langmuir, and Temkin isotherm models were considered to analyse the kinetics and isotherms of NH_4^+-N adsorption using biosolids-derived biochar, as shown in Table 2 (Zhou et al., 2017). The linear and non-linear regressions were performed in a Microsoft Excel spreadsheet to fit the adsorption kinetic and isotherm models with experimental adsorption data. The coefficient of correlation (R^2) was also determined from the regression analysis to explore the applicability of isotherm and kinetic models and to explain the adsorption mechanism.

3. Results and discussion

3.1. Characterisation of adsorbents

BET surface area of adsorbents was determined as in this order: activated carbon (1000 m^2 g^{-1}) > zeolite (609 m^2 g^{-1}) > biosolids biochar produced at 700 °C (90 m^2 g^{-1}) > biomass biochar produced at 500 °C (51 m^2 g^{-1}) > cation exchange resin (35 m^2 g^{-1}) > biosolids biochar produced at 500 °C (32 m^2 g^{-1}). These values demonstrate that all of these porous materials can be morphologically appropriate media to embed adsorbate molecules. However, the density of functional groups with its direct influence on the electron-cloud distribution of the surface did not follow the same order. The FTIR analysis results (Fig. 1) for all adsorbents used in this study revealed that cation exchange resin presented multiple functional groups on its surface for NH_4^+-N

Table 2
Kinetic and isotherm models considered in this study.

Model type	Model name	Equation
Kinetic model	Pseudo first order	$\frac{dQ_t}{dt} = k_1(Q_e - Q_t)$
	Pseudo second order	$\frac{dQ_t}{dt} = k_2(Q_e - Q_t)^2$
	Elovich	$\frac{dQ_t}{dt} = aexp(-bQ_t)$
	Intra-particle diffusion	$Q_t = K_i t^{1/2} + C$
Isotherm model	Freundlich	$Q_e = K_f C_e^{1/n}$
	Langmuir	$Q_e = Q_m K_L \frac{C_e}{1 + K_L C_e}$
	Temkin	$Q_e = \frac{RT}{b_T} ln\,(A\,C_e)$

Q_e = adsorption capacity at equilibrium time, Q_t = adsorption capacity at time t, K_1 = rate constant of pseudo-first order, K_2 = rate constant of pseudo-second order, a = rate constant of chemisorption, b = constant of the surface coverage, K_i = intra-particle diffusion rate constant, t = time, C = a constant, K_f = Freundlich constant, C_e = equilibrium concentration, Q_m = maximum adsorption capacity, K_L = Langmuir constant, R = universal gas constant, T = temperature (Kelvin), b_T = Temkin constant and A = equilibrium bond constant.

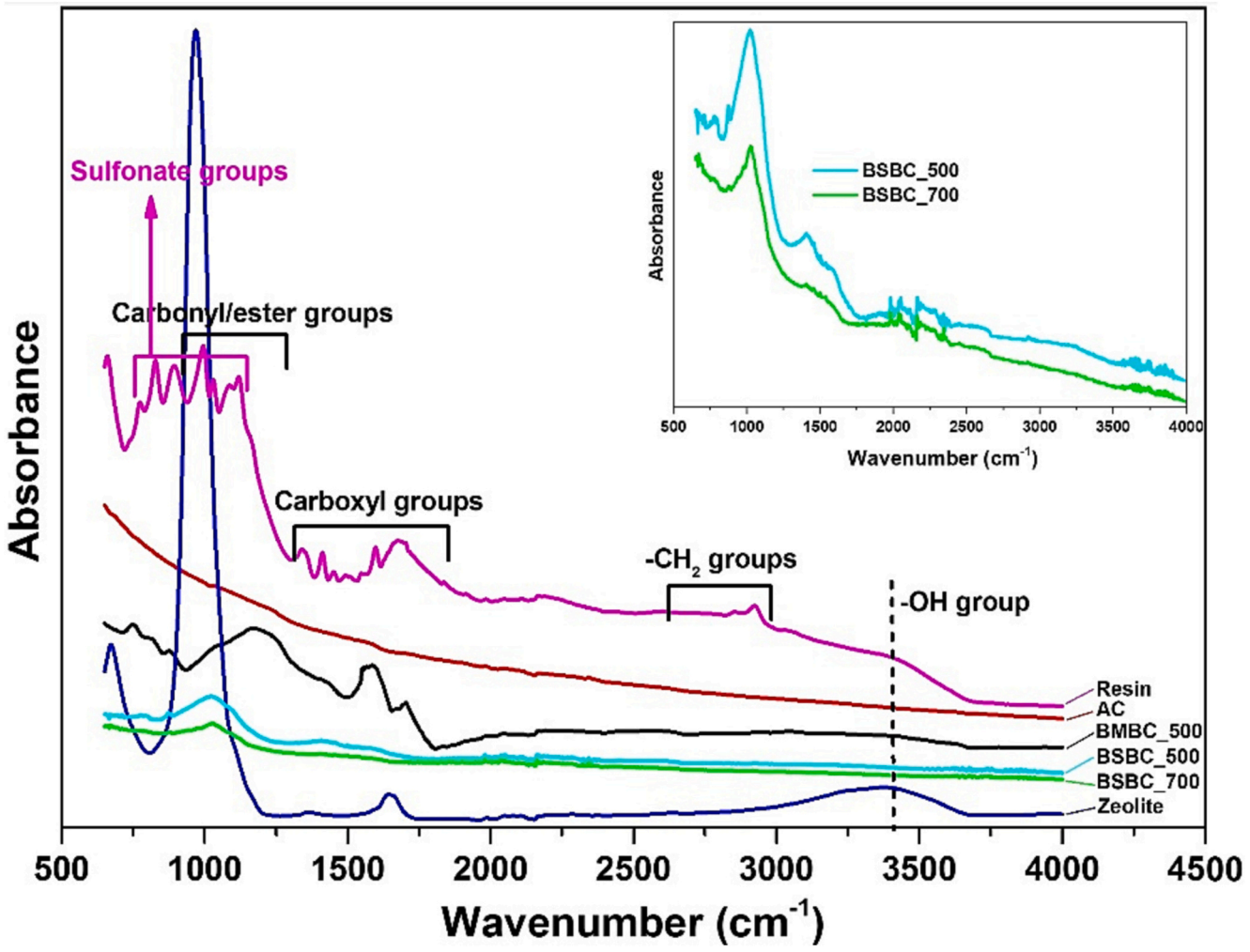

Fig. 1. FTIR analysis of biomass/biosolids-derived biochars and other known adsorbents.

adsorption. In contrast, activated carbon had no distinctive functional groups on its surface. This might be due to the decomposition of all functional groups during the preparation (i.e., thermal treatment) of activated carbon.

Sulfonated, carbonyl/ester, and carboxyl groups were the major peaks of cation exchange resin adsorbent. The resin is strongly acidic given the presence of the sulfonic acid ($-SO_3H$) functional group, thus potentially can be a good candidate for NH_4^+-N adsorption due to the exchange of H^+ ion in $-SO_3H$ with the ammonium ion, as sulfonic acid group acts as a proton donor. The ion exchange capacity for the $-SO_3H$ group was found to be relatively high because the sulphonic acid group readily dissociates at neutral pH (Castillo-Cervantes et al., 2019) to exchange the H^+ ion with the ammonium ion. No further cation exchange is expected to happen on a site after ammonium is adsorbed. There was also a high absorbance for carbonyl (C═O bond) followed by carboxyl (C(=O)OH) groups. According to density functional theory, the carbonyl group was found to have a higher adsorption energy value and shorter bond distance for ammonium ion adsorption (Yin et al., 2022). This also clearly underlines the dependence of NH_4^+-N adsorption on the type of functional group.

Zeolite also possessed a few distinctive functional groups at wavenumbers of 3450, 1621, 1015 and 705 cm^{-1}, attributed to O—H stretching vibration, O—H bending vibration of H_2O molecules in the zeolite voids, asymmetric and symmetric stretch vibration of T-O-T bonds where T is the tetrahedrally bonded Si or Al, respectively (Bakatula et al., 2015; Wiśniewska et al., 2020). As seen, the inherent functional group of zeolites may need to exclusively be designed for ammonium adsorption because only its hydroxyl group can play a role in adsorption.

The functional groups of biochars produced in the present work are consistent with the other biochars in the literature (L. Liu et al., 2021a; Reza et al., 2020). Biomass-derived biochar had two peaks at around 1220 and 1550–1710 cm^{-1}, which are ascribed to -CO, -C=C bonds in carbonyl and carboxylic functional groups. Depolymerisation and dehydration reactions are the main pathways during the pyrolysis of lignocellulosic biomass through which C═C bonds, carbonyl and carboxylic functional groups are formed (Chia et al., 2012). In biosolids-derived biochar, a peak was observed between 1100 and 1000 cm^{-1} within the fingerprint region, which can be assigned to the C-O-C bond stretching of the lignin ethers (Pattnaik et al., 2018). The peak in the range of wavenumbers from 1480 to 1410 cm^{-1} belongs to the stretching of C—H as a result of cellulose and hemicellulose deformation (Tayibi et al., 2020). The study also compared the intensity of peaks for the biosolids biochar derived at 500 and 700 °C and showed that the absorbance value for all peaks diminished at higher temperatures which is in accordance with the previous study (Reza et al., 2020). Despite of increasing the BET surface area by almost three times (90 vs 32 m^2g^{-1}), the useful functional groups were destroyed at 700 °C compared to those at 500 °C. Biosolids biochars also had a number of small peaks between 2000 and 2500 cm^{-1} attributed to -C=O stretching bond in the ketene (Reza et al., 2019).

3.2. Benchmarking of biosolids-derived biochar with other adsorbents

Fig. 2 compares the performance of various adsorbents for ammonium uptake at two initial concentrations of 5 and 50 mg L^{-1} and contact times of 5 and 24 h. As expected, resin outperformed its counterparts in removing ammonium from synthetic wastewater given its desired sulfonated functional groups followed by zeolite and biochar. The adsorption mechanisms of ammonium mainly include ion exchange between NH_4^+-N and functional groups (sulfonate groups, hydroxyl groups, and protons of C—H) on the biochar surface, complexation of NH_4^+-N in carboxyl groups, and electrostatic attraction (R. Liu et al., 2021b). Very interestingly, activated carbon with the highest BET surface area showed the lowest affinity for ammonium uptake, clearly revealing that the capacity of adsorption entirely depends on the type and density of functional groups rather than the surface area.

In all experiments, higher initial concentration favoured the adsorption performance. The improved performance in the case of resin was more distinct compared with the other five adsorbents, with its adsorption capacity reaching nearly 4 from 0.5 mg g^{-1}. The higher initial concentration provides a higher concentration difference between the solution and the adsorbent surface or an increased affinity towards active sites (Delaila Tumin et al., 2008). In other words, a higher driving force is provided at a higher initial ammonium concentration, helping overcome the mass transfer resistances of the adsorbate molecules from the aqueous phase to the active sites in the solid phase (Pandey et al., 2010). Moreover, this suggests that the adsorption of ammonium from non-diluted wastewater is preferred, meaning that ammonium is better to be adsorbed at the source level i.e., urinals rather than centralized wastewater treatment plant. It is noteworthy that a higher adsorption capacity means a lower consumption of adsorbent, thereby lowering both operating and capital costs.

Lastly, it is evident from Fig. 2a that extending the contact time from 5 to 24 h has a dramatic effect on the adsorption using biochar, with a little effect for resin and zeolite. This should not be misunderstood that adsorption by resin or zeolite was not time-dependent. The results demonstrated that the adsorption reached its equilibrium in <5 h and at a much faster rate, therefore prolonging the experiment would be unreasonable. For adsorption processes with long contact time similar to adsorption by biochar, normally the intra-particle diffusion may partially or wholly dominate the uptake mechanism (Chen et al., 2021). Therefore, the ammonium ions took a longer time to diffuse through the pores of biochar due to the slow pore diffusion process (Cui et al., 2016). It can also be observed that the nitrogen adsorption using biochar derived from biosolids is in accordance with previous literature (Fig. 2b) (Carey et al., 2015; Han et al., 2021; Tang et al., 2019).

3.3. Effect of initial concentration and adsorption time

Fig. 3 exhibits the dependence of the adsorption capacity of biosolids-derived biochar at 500 °C (BSBC_500) on the initial concentration of NH_4^+-N and contact time. As discussed in the previous section, typically a higher initial concentration and a longer contact time would lead to a higher adsorption capacity. For the initial concentration in the range of 5 to 100 mg L^{-1} (Fig. 3a), there was a logarithmic correlation between capacity and initial concentration, where the adsorption capacity appeared to reach a plateau at a higher concentration. This highlights the possibility of the occurrence of multi-layer adsorption where the active sites get nearly saturated at an increased initial concentration of 80 mg L^{-1} and further increase to 100 mg L^{-1} cannot substantially improve the capacity comparable to the previous intervals. Removal efficiency constantly decreased as the initial concentration increased which is expected as there will be more NH_4^+-N molecules in the solution that were not adsorbed.

On the effect of contact time, as it is clear from Fig. 3b, the capacity gradually increased with time until it reached the equilibrium state after approximately 24 h from the start of the run. The higher initial adsorption was associated with a large number of vacant active surface sites of biochar during the initial stage which gradually reduced with adsorption time. This distinctly highlights the importance of diffusion of NH_4^+-N molecules into the biochar porous structure. If the BET surface area could be increased by maintaining the density of functional groups on the surface, its capacity for ammonium adsorption could also meaningfully increase. To accelerate the process, the active sites must come to the surface and be readily accessible and available for adsorption. It is also worth noting that the capacity after 12 h was almost 90 % of the equilibrium capacity. One should decide here whether to continue the process for another 12 h to attain the full capacity. Economic considerations also play a key role in this situation as prolonging the run can double the capital investment.

3.4. Effect of heavy metal and drug on nitrogen NH_4^+-N adsorption

In order to also investigate the effect of the presence of other adsorbate molecules in the solution along with ammonium, Zinc, and Caffeine with a concentration of 0.05 mg L^{-1} (Hubeny et al., 2021) were added to the solution as model compounds. Fig. 4 shows that the variation of nitrogen adsorption in the presence of Zinc and Caffeine using biosolids-derived biochar was as low as ~3–4 %. This is mainly due to

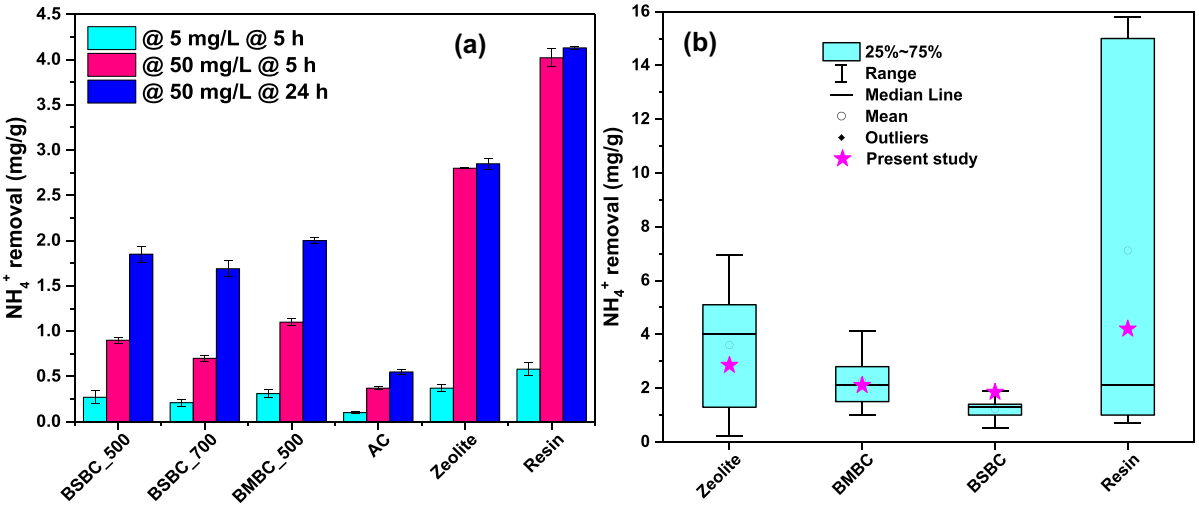

Fig. 2. (a) Adsorption of ammonium from synthetic wastewater using various adsorbents and (b) comparison of the current study with previous literature (Box chart: literature data).

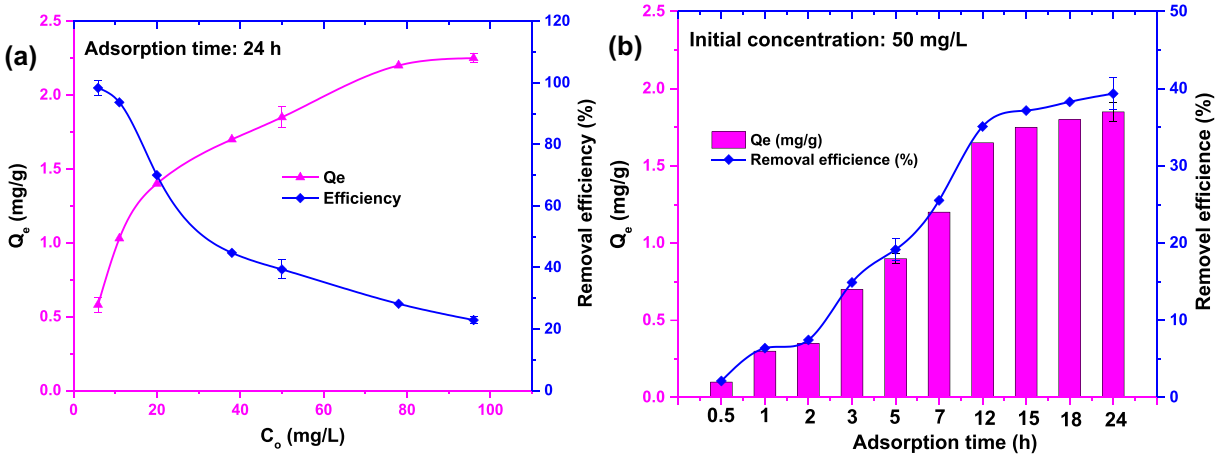

Fig. 3. The effect of (a) initial concentration and (b) adsorption time on the adsorption capacity of BSBC_500.

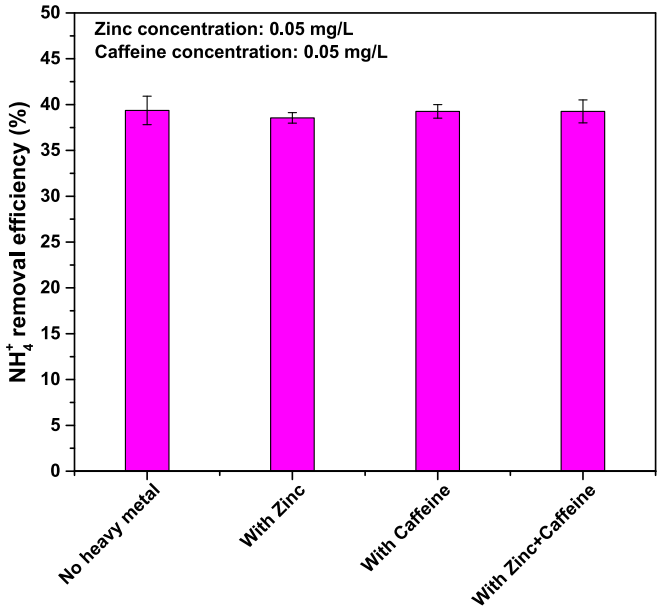

Fig. 4. The effect of the addition of Zinc and Caffeine on the capacity of BSBC_500 for ammonium adsorption.

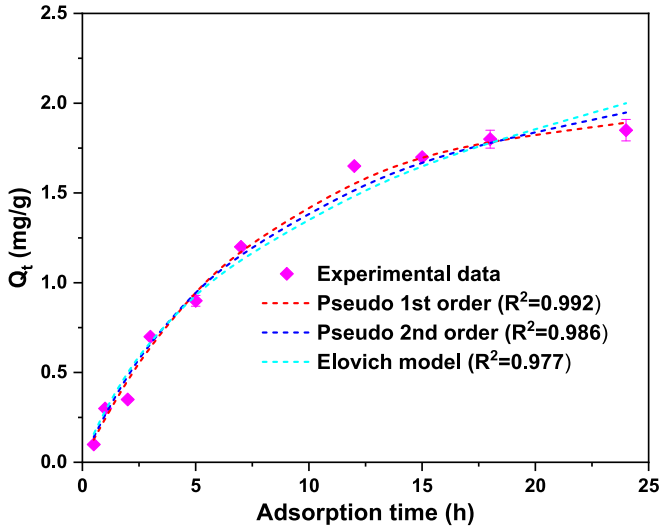

Fig. 5. Kinetic experimental data and fitting with known kinetic models.

the very low concentration of these additional pollutants which cannot compete with ammonium to occupy the active sites. Although the main components available in the wastewater (Table 1) were added to the solution, further study on the identification of other potential adsorbate molecules including antibiotics, dyestuff, and other heavy metals is still needed. This would provide a more comprehensive picture of to what extent ammonium is competitively adsorbed.

3.5. Kinetics of NH_4^+-N adsorption by BSBC_500

The kinetic experimental data is provided in Fig. 5 for a range of 0 to 24 h, where it follows a logarithmic trend. The regression analysis results revealed that all three kinetic models can acceptably fit the experimental data, however pseudo first order model was in the best agreement with the experimental data with an R^2 value of 0.992. Table 3 shows the parameters of three NH_4^+-N adsorption kinetic models. The pseudo first-order model assumes that NH_4^+-N adsorption using biosolids-derived biochar can occur in two stages, such as an external film layer adsorption followed by an intraparticle diffusion adsorption. According to the pseudo first-order model, at any time during the process, the rate of adsorption is directly proportional to the distance from equilibrium i.e., the difference of saturation capacity and capacity at time t (Rodrigues and Silva, 2016). The adsorption kinetic parameters, such as adsorption rate, adsorption rate constant and equilibrium adsorption capacity will be helpful for designing the column for continuous adsorption and scale-up process development.

Table 3
Kinetic parameters for NH_4^+-N adsorption on BSBC_500.

Model	Parameter (Unit)	Value	R^2
1st order	Q_e (mg g^{-1})	1.97	0.992
	k_1 (1/h)	0.13	
2nd order	Q_e (mg g^{-1})	2.68	0.982
	k_2 (g/mg.h)	0.04	
Elovich	a (mg g^{-1}.h)	0.35	0.977
	b (g/mg)	1.20	

The intra-particle diffusion model was also investigated for a further in-depth understanding of the mechanism of ammonium ion's movement towards biochar adsorbent and the rate-controlling step affecting the NH_4^+-N adsorption kinetics. It is evident in Fig. 6a that the single-stage model fitting curve ($R^2 = 0.961$) did not pass through the origin, indicating that the particle diffusion was not the only rate-controlling mechanism. The other mechanisms such as external surface layer

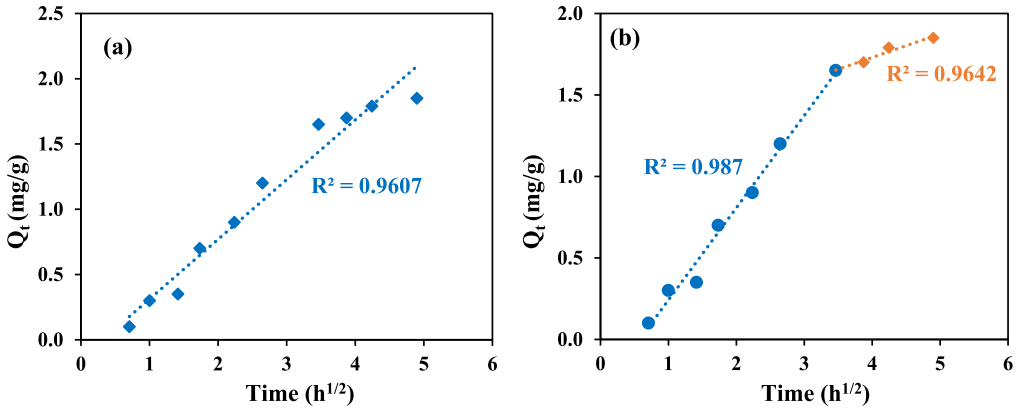

Fig. 6. Intra-particle diffusion model fitting with experimental data (a) single stage fitting and (b) multi-stage fitting.

diffusion can also affect the rate-controlling step. Fig. 6b shows the multilinearity of adsorption, indicating that the adsorption of NH_4^+-N occurred in two stages. The regression coefficient of the 1st and 2nd stages was 0.987 and 0.964, respectively which was also in agreement with that the rate-controlling step was governed by two adsorption mechanisms. The first sharp stage (up to 12 h) was attributed to the external surface diffusion mechanism (Abodif et al., 2020), indicating the interaction of functional groups of biochar's external surface with NH_4^+-N. The 2nd stage was the gradual adsorption stage, where the intraparticle diffusion was the rate-controlling step for NH_4^+-N adsorption by biochar. This model provides insightful information on the dynamics of NH_4^+-N adsorption.

3.6. NH_4^+-N adsorption isotherms for BSBC_500

As shown in Fig. 7, the values of ammonium adsorption using biosolids-derived biochar at various initial concentrations were determined. Adsorption isotherm data present how the adsorption process moves forwards and demonstrates how effectively an adsorbent can eliminate the adsorbate molecules from an aqueous solution (Marzbali et al., 2016). The efficiency of BSBC_500 adsorbent to remove NH_4^+-N ions from synthetic wastewater was investigated via the trend of adsorption isotherm data.

The results of the linear regression of the above-mentioned models revealed the model with the best fit. As can be seen from Fig. 7, the experimental data were in better agreement with the Freundlich isotherm model with an R^2 value of 0.986. This would mean that BSBC_500 has a heterogeneous surface on which active sites have varied affinities towards NH_4^+-N adsorption. Table 4 shows the parameters of three models for the NH_4^+-N isothermal adsorption data. Temkin isotherm model could also well fit the experimental data, suggesting that most probably multilayer adsorption is taking place. This was also evident from the inferior fit of the Langmuir isotherm model, ruling out the monolayer adsorption hypothesis.

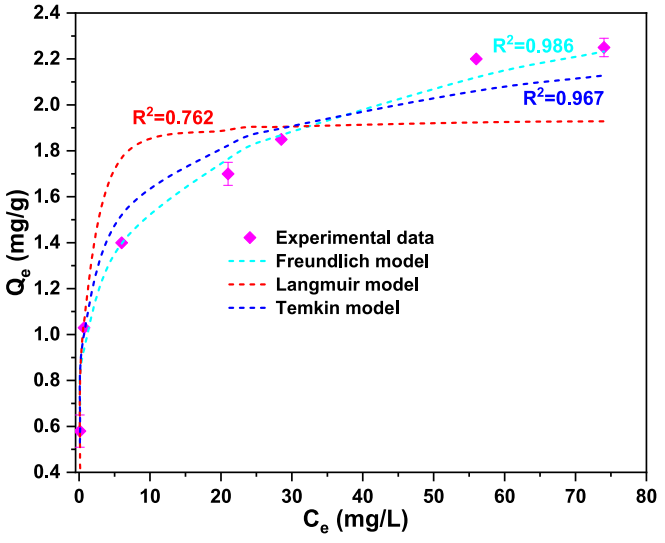

Fig. 7. Experimental data for isotherm study and fitting with known isotherm models.

4. Future directions and business recommendations

The current study explored a promising pathway for NH_4^+-N capture from wastewater in the WWTP using biochar produced from the WWTP's own biosolids in the plant premises. Therefore, the following objectives can be logical routes to continue the present study and to develop a scale-up adsorption process.

- Optimisation of process parameters (i.e., biochar dosage, concentration, pH) for nitrogen adsorption using biosolids-derived biochar.
- Exploring the cost-effective routes of functionalising the biochar for retaining high functional groups and increasing cation exchange capacity.
- Studying the effect of high concentrations of heavy metals and drugs and other pollutants.
- Derivation of kinetics and isotherms for nitrogen recovery from real wastewater.
- Biochar bed adsorption column study and developing a detailed techno-economic analysis for a hypothetical or real WWTP.
- Potential applicability of nitrogen-loaded biochar as fertiliser.

5. Conclusions

This paper benchmarks the NH_4^+-N adsorption by biosolids biochar with zeolite, resin, activated carbon and biomass biochar. At an initial NH_4^+-N concentration of 50 mg L^{-1} with 24 h adsorption time, biosolids-derived biochar adsorbed 1.8 mg NH_4^+-N g^{-1} adsorbent which was nearly half of the cation exchange resin and zeolite. External surface

Table 4
Isotherm parameters for NH_4^+-N adsorption on BSBC_500.

Model	Parameter (Unit)	Value	R^2
Freundlich	K_f (L/g)	1.00	0.986
	n	5.35	
Langmuir	Q_m (mg g^{-1})	1.94	0.762
	K_L (L/g)	1.69	
Temkin	b (kJ/mol)	10.15	0.967
	A (L/g)	89.68	

layer diffusion was the governing step in the early stage of NH_4^+-N adsorption while intra-particle diffusion was the main mechanism in the later stage of adsorption. Isotherm data modelling also showed the heterogeneity of biosolids biochar surface and the occurrence of multi-layer adsorption. The NH_4^+-N-loaded biochar can be a potential slow-release fertiliser for agricultural purposes as it will reduce the consumption of synthetic nitrogen-based fertiliser to a certain extent, which is an energy and emission-intensive approach. Therefore, biosolids-derived biochar can be a future attractive option for NH_4^+-N recovery from wastewater in a circular way.

CRediT authorship contribution statement

Pobitra Halder: Conceptualization, Methodology, Formal analysis, Investigation, Writing – original draft, Visualization, Writing – review & editing. **Mojtaba Hedayati Marzbali:** Writing – original draft, Writing – review & editing. **Savankumar Patel:** Visualization, Writing – review & editing. **Graeme Short:** Funding acquisition, Writing – review & editing. **Aravind Surapaneni:** Funding acquisition, Writing – review & editing. **Rajender Gupta:** Writing – review & editing. **Kalpit Shah:** Supervision, Conceptualization, Resources, Writing – review & editing.

Declaration of competing interest

The authors declare that they have no known competing financial interests or personal relationships that could have appeared to influence the work reported in this paper.

Data availability

Data will be made available on request.

Acknowledgments

The authors would like to acknowledge the support received from South East Water Corporation, Australia under the Australian Post-graduate Research (APR) internship program. The support from technical officers of Chemical Engineering School laboratories at RMIT University is also greatly appreciated. This APR internship program was administrated and facilitated by Mr. Zak Blayney and Mr. Justin Mabbutt, whose help is also much appreciated.

References

Abodif, A.M., Abodif, A.M., Meng, L., Ma, S., Ahmed, A.S.A., Belvett, N., Wei, Z.Z., Ning, D., 2020. Mechanisms and models of adsorption: TiO2-supported biochar for removal of 3,4-dimethylaniline. ACS Omega 5, 13630–13640. https://doi.org/10.1021/acsomega.0c00619.

Al Nami, S.Y., Hossan, A., 2023. Adsorption of triclosan from aqueous solutions via novel metal–organic framework: adsorption isotherms, kinetics, and optimization via Box-Behnken design. J. Mol. Liq. 382 https://doi.org/10.1016/j.molliq.2023.122065.

AMPC, 2022. AMPC wastewater management fact sheet series. In: Nitrogen Removal.

Bai, X., Li, Z., Zhang, Y., Ni, J., Wang, X., Zhou, X., 2018. Recovery of ammonium in urine by biochar derived from faecal sludge and its application as soil conditioner. Waste Biomass Valorization 9, 1619–1628. https://doi.org/10.1007/s12649-017-9906-0.

Bakatula, E.N., Mosai, A.K., Tutu, H., 2015. Removal of uranium from aqueous solutions using ammonium-modified zeolite. S. Afr. J. Chem. 68, 165–171. https://doi.org/10.17159/0379-4350/2015/V68A23.

Beckinghausen, A., Reynders, J., Merckel, R., Wu, Y.W., Marais, H., Schwede, S., 2020. Post-pyrolysis treatments of biochars from sewage sludge and A. mearnsii for ammonia (NH4-n) recovery. Appl. Energy 271, 115212. https://doi.org/10.1016/J.APENERGY.2020.115212.

Bhatnagar, A., Sillanpää, M., 2011. A review of emerging adsorbents for nitrate removal from water. Chem. Eng. J. 168, 493–504. https://doi.org/10.1016/J.CEJ.2011.01.103.

Carey, D.E., McNamara, P.J., Zitomer, D.H., 2015. Biochar from pyrolysis of biosolids for nutrient adsorption and turfgrass cultivation. Water Environ. Res. 87, 2098–2106. https://doi.org/10.2175/106143015X14362865227391.

Castillo-Cervantes, J.N., Lijanova, I.V., Likhanova, N.V., Olivares-Xometl, O., Navarrete-Bolaños, J., Gómora-Herrera, D.R., 2019. Extraction of reactive dyes from aqueous solutions by halogen-free ionic liquids. Color. Technol. 135, 417–426. https://doi.org/10.1111/cote.12429.

Chang, J.H., Sivasubramanian, P.D., Di Dong, C., Kumar, M., 2023. Study on adsorption of ammonium and nitrate in wastewater by modified biochar. Bioresour. Technol. Rep. 21, 101346 https://doi.org/10.1016/j.biteb.2023.101346.

Chen, Z., Wang, X., Chen, X., Yang, Y., Gu, X., 2019. Pilot study of nitrogen removal from landfill leachate by stable nitritation-denitrification based on zeolite biological aerated filter. Waste Manag. 100, 161–170. https://doi.org/10.1016/J.WASMAN.2019.09.020.

Chen, M., Wang, F., Zhang, D.-li, Yi, W. Ming, Liu, Y., 2021. Effects of acid modification on the structure and adsorption NH4+-N properties of biochar. Renew. Energy 169, 1343–1350. https://doi.org/10.1016/J.RENENE.2021.01.098.

Chia, C.H., Gong, B., Joseph, S.D., Marjo, C.E., Munroe, P., Rich, A.M., 2012. Imaging of mineral-enriched biochar by FTIR, Raman and SEM–EDX. Vib. Spectrosc. 62, 248–257. https://doi.org/10.1016/J.VIBSPEC.2012.06.006.

Cui, X., Hao, H., Zhang, C., He, Z., Yang, X., 2016. Capacity and mechanisms of ammonium and cadmium sorption on different wetland-plant derived biochars. Sci. Total Environ. 539, 566–575. https://doi.org/10.1016/J.SCITOTENV.2015.09.022.

Dai, Y., Wang, W., Lu, L., Yan, L., Yu, D., 2020. Utilization of biochar for the removal of nitrogen and phosphorus. J. Clean. Prod. https://doi.org/10.1016/j.jclepro.2020.120573.

Delaila Tumin, N., Chuah, A.L., Zawani, Z., Rashid, S.A., 2008. Adsorption of copper from aqueous solution by Elais Guineensis kernel activated carbon. J. Eng. Sci. Technol. 3, 180–189.

Du, R., Peng, Y., Cao, S., Wang, S., Wu, C., 2015. Advanced nitrogen removal from wastewater by combining anammox with partial denitrification. Bioresour. Technol. 179, 497–504. https://doi.org/10.1016/J.BIORTECH.2014.12.043.

Han, B., Butterly, C., Zhang, W., He, J. zheng, Chen, D., 2021. Adsorbent materials for ammonium and ammonia removal: a review. J. Clean. Prod. 283, 124611 https://doi.org/10.1016/J.JCLEPRO.2020.124611.

Hubeny, J., Harnisz, M., Korzeniewska, E., Buta, M., Zieliński, W., Rolbiecki, D., Giebułtowicz, J., Nałęcz-Jawecki, G., Płaza, G., 2021. Industrialization as a source of heavy metals and antibiotics which can enhance the antibiotic resistance in wastewater, sewage sludge and river water. PLoS One 16. https://doi.org/10.1371/JOURNAL.PONE.0252691.

Kundu, S., Pramanik, B.K., Halder, P., Patel, S., Ramezani, M., Khairul, M.A., Marzbali, M.H., Paz-Ferreiro, J., Crosher, S., Short, G., Surapaneni, A., Bergmann, D., Shah, K., 2022. Source and central level recovery of nutrients from urine and wastewater: a state-of-art on nutrients mapping and potential technological solutions. J. Environ. Chem. Eng. 10, 107146 https://doi.org/10.1016/J.JECE.2022.107146.

Li, S., Barreto, V., Li, R., Chen, G., Hsieh, Y.P., 2018. Nitrogen retention of biochar derived from different feedstocks at variable pyrolysis temperatures. J. Anal. Appl. Pyrolysis 133, 136–146. https://doi.org/10.1016/J.JAAP.2018.04.010.

Li, B., Jing, F., Hu, Z., Liu, Y., Xiao, B., Guo, D., 2021. Simultaneous recovery of nitrogen and phosphorus from biogas slurry by Fe-modified biochar. J. Saudi Chem. Soc. 25, 101213 https://doi.org/10.1016/J.JSCS.2021.101213.

Liu, R., Yang, Z., Wang, G., Xian, J., Li, T., Pu, Y., Jia, Y., Zhou, W., Cheng, Z., Zhang, S., Xiang, G., Xu, X., 2021a. Simultaneous removal of ammonium and phosphate in aqueous solution using Chinese herbal medicine residues: mechanism and practical performance. J. Clean. Prod. 313, 127945 https://doi.org/10.1016/J.JCLEPRO.2021.127945.

Liu, L., Yue, T., Liu, R., Lin, H., Wang, D., Li, B., 2021b. Efficient absorptive removal of Cd(II) in aqueous solution by biochar derived from sewage sludge and calcium sulfate. Bioresour. Technol. 336, 125333 https://doi.org/10.1016/J.BIORTECH.2021.125333.

Marzbali, Mojtaba Hedayati, Esmaieli, M., Abolghasemi, H., Marzbali, Mostafa Hedayati, 2016. Tetracycline adsorption by H3PO4-activated carbon produced from apricot nut shells: a batch study. Process Saf. Environ. Prot. 102, 700–709. https://doi.org/10.1016/J.PSEP.2016.05.025.

Nayak, A., Bhushan, B., Gupta, V., Kotnala, S., 2021. Fabrication of microwave assisted biogenic magnetite-biochar nanocomposite: a green adsorbent from jackfruit peel for removal and recovery of nutrients in water sample. J. Ind. Eng. Chem. 100, 134–148. https://doi.org/10.1016/J.JIEC.2021.05.028.

Pandey, P.K., Sharma, S.K., Sambi, S.S., 2010. Kinetics and equilibrium study of chromium adsorption on zeoliteNaX. Int. J. Environ. Sci. Technol. 7, 395–404. https://doi.org/10.1007/BF03326149, 2 7.

Patel, S., Kundu, S., Halder, P., Rickards, L., Paz-Ferreiro, J., Surapaneni, A., Madapusi, S., Shah, K., 2019. Thermogravimetric analysis of biosolids pyrolysis in the presence of mineral oxides. Renew. Energy 141, 707–716. https://doi.org/10.1016/j.renene.2019.04.047.

Pattnaik, D., Kumar, S., Bhuyan, S.K., Mishra, S.C., 2018. Effect of carbonization temperatures on biochar formation of bamboo leaves. IOP Conf. Ser. Mater. Sci. Eng. 338, 012054 https://doi.org/10.1088/1757-899X/338/1/012054.

Pramanik, B.K., Islam, M.A., Asif, M.B., Roychand, R., Pramanik, S.K., Shah, K., Bhuiyan, M., Hai, F., 2020. Emerging investigator series: phosphorus recovery from municipal wastewater by adsorption on steelmaking slag preceding forward osmosis: an integrated process. Environ. Sci. (Camb.) 6, 1559–1567. https://doi.org/10.1039/D0EW00187B.

Preisner, M., Neverova-Dziopak, E., Kowalewski, Z., 2021. Mitigation of eutrophication caused by wastewater discharge: a simulation-based approach. Ambio 50, 413–424. https://doi.org/10.1007/s13280-020-01346-4.

Pronk, W., Koné, D., 2009. Options for urine treatment in developing countries. Desalination 248, 360–368. https://doi.org/10.1016/J.DESAL.2008.05.076.

Rahimi, S., Modin, O., Mijakovic, I., 2020. Technologies for biological removal and recovery of nitrogen from wastewater. Biotechnol. Adv. 43, 107570 https://doi.org/10.1016/J.BIOTECHADV.2020.107570.

Reza, M.S., Islam, S.N., Afroze, S., Abu Bakar, M.S., Sukri, R.S., Rahman, S., Azad, A.K., 2019. Evaluation of the bioenergy potential of invasive Pennisetum purpureum through pyrolysis and thermogravimetric analysis. Energy Ecol. Environ. 5, 118–133. https://doi.org/10.1007/S40974-019-00139-0, 2 5.

Reza, M.S., Afroze, S., Bakar, M.S.A., Saidur, R., Aslfattahi, N., Taweekun, J., Azad, A.K., 2020. Biochar characterization of invasive Pennisetum purpureum grass: effect of pyrolysis temperature. Biochar 2, 239–251. https://doi.org/10.1007/S42773-020-00048-0.

Rodrigues, A.E., Silva, C.M., 2016. What's wrong with Lagergreen pseudo first order model for adsorption kinetics? Chem. Eng. J. 306, 1138–1142. https://doi.org/10.1016/J.CEJ.2016.08.055.

Safie, N.N., Zahrim, A.Y., 2021. Recovery of nutrients from sewage using zeolite-chitosan-biochar adsorbent: current practices and perspectives. J. Water Process. Eng. 40, 101845 https://doi.org/10.1016/J.JWPE.2020.101845.

Sánchez, A.S., Martins, G., 2021. Nutrient recovery in wastewater treatment plants: comparative assessment of different technological options for the metropolitan region of Buenos Aires. J. Water Process. Eng. 41, 102076 https://doi.org/10.1016/J.JWPE.2021.102076.

Shang, L., Xu, H., Huang, S., Zhang, Y., 2018. Adsorption of ammonium in aqueous solutions by the modified biochar and its application as an effective N-fertilizer. Water Air Soil Pollut. 229 https://doi.org/10.1007/s11270-018-3956-1.

Simha, P., Zabaniotou, A., Ganesapillai, M., 2018. Continuous urea–nitrogen recycling from human urine: a step towards creating a human excreta based bio–economy. J. Clean. Prod. 172, 4152–4161. https://doi.org/10.1016/J.JCLEPRO.2017.01.062.

Širić, I., Eid, E.M., Taher, M.A., El-Morsy, M.H.E., Osman, H.E.M., Kumar, P., Adelodun, B., Fayssal, S.A., Mioč, B., Andabaka, Ž., Goala, M., Kumari, S., Bachheti, A., Choi, K.S., Kumar, V., 2022. Combined use of spent mushroom substrate biochar and PGPR improves growth, yield, and biochemical response of cauliflower (Brassica oleracea var. botrytis): a preliminary study on greenhouse cultivation. Horticulture 8, 1–14. https://doi.org/10.3390/horticulturae.

Tang, Y., Alam, M.S., Konhauser, K.O., Alessi, D.S., Xu, S., Tian, W.J., Liu, Y., 2019. Influence of pyrolysis temperature on production of digested sludge biochar and its application for ammonium removal from municipal wastewater. J. Clean. Prod. 209, 927–936. https://doi.org/10.1016/J.JCLEPRO.2018.10.268.

Tarpeh, W.A., Wald, I., Wiprächtiger, M., Nelson, K.L., 2018. Effects of operating and design parameters on ion exchange columns for nutrient recovery from urine. Environ. Sci. (Camb.) 4, 828–838. https://doi.org/10.1039/C7EW00478H.

Tayibi, S., Monlau, F., Fayoud, N. elhouda, Oukarroum, A., Zeroual, Y., Hannache, H., Barakat, A., 2020. One-pot activation and pyrolysis of Moroccan *Gelidium sesquipedale* red macroalgae residue: production of an efficient adsorbent biochar. Biochar 1, 401–412. https://doi.org/10.1007/S42773-019-00033-2, 2020 1:4.

van der Hoek, J.P., Duijff, R., Reinstra, O., 2018. Nitrogen recovery from wastewater: possibilities, competition with other resources, and adaptation pathways. Sustainability 10, 4605. https://doi.org/10.3390/SU10124605. Vol. 10, Page 4605.

Wang, X., Guo, Z., Hu, Z., Zhang, J., 2020. Recent advances in biochar application for water and wastewater treatment: a review. PeerJ 8, e9164. https://doi.org/10.7717/PEERJ.9164/FIG-3.

Wang, H., Liu, R., Chen, Q., Mo, Y., Zhang, Y., 2022. Biochar-supported starch/chitosan-stabilized nano-iron sulfide composites for the removal of lead ions and nitrogen from aqueous solutions. Bioresour. Technol. 347, 126700 https://doi.org/10.1016/J.BIORTECH.2022.126700.

Wiśniewska, M., Urban, T., Chibowski, S., Fijałkowska, G., Medykowska, M., Nosal-Wiercińska, A., Franus, W., Panek, R., Szewczuk-Karpisz, K., 2020. Investigation of adsorption mechanism of phosphate(V) ions on the nanostructured Na-a zeolite surface modified with ionic polyacrylamide with regard to their removal from aqueous solution. Appl. Nanosci. 10, 4475–4485. https://doi.org/10.1007/S13204-020-01397-9/TABLES/2.

Xu, K., Lin, F., Dou, X., Zheng, M., Tan, W., Wang, C., 2018. Recovery of ammonium and phosphate from urine as value-added fertilizer using wood waste biochar loaded with magnesium oxides. J. Clean. Prod. 187, 205–214. https://doi.org/10.1016/J.JCLEPRO.2018.03.206.

Xue, S., Zhang, X., Ngo, H.H., Guo, W., Wen, H., Li, C., Zhang, Y., Ma, C., 2019. Food waste based biochars for ammonia nitrogen removal from aqueous solutions. Bioresour. Technol. 292, 121927 https://doi.org/10.1016/J.BIORTECH.2019.121927.

Yin, Q., Zhang, B., Wang, R., Zhao, Z., 2017. Biochar as an adsorbent for inorganic nitrogen and phosphorus removal from water: a review. Environ. Sci. Pollut. Res. 24, 26297–26309. https://doi.org/10.1007/S11356-017-0338-Y/TABLES/2.

Yin, Q., Si, L., Wang, R., Zhao, Z., Li, H., Wen, Z., 2022. DFT study on the effect of functional groups of carbonaceous surface on ammonium adsorption from water. Chemosphere 287, 132294. https://doi.org/10.1016/J.CHEMOSPHERE.2021.132294.

Yu, C., 2022. Recovery of NH4+-N and PO43–P from urine using sludge-derived biochar as a fertilizer: performance and mechanism. RSC Adv. 12, 4224–4233. https://doi.org/10.1039/d1ra08558a.

Zhao, Z., Wang, B., Feng, Q., Chen, M., Zhang, X., Zhao, R., 2022. Recovery of nitrogen and phosphorus in wastewater by red mud-modified biochar and its potential application. Sci. Total Environ. 160289 https://doi.org/10.1016/J.SCITOTENV.2022.160289.

Zhou, Y., Liu, X., Xiang, Y., Wang, P., Zhang, J., Zhang, F., Wei, J., Luo, L., Lei, M., Tang, L., 2017. Modification of biochar derived from sawdust and its application in removal of tetracycline and copper from aqueous solution: adsorption mechanism and modelling. Bioresour. Technol. 245, 266–273. https://doi.org/10.1016/j.biortech.2017.08.178.